International Journal of
INTELLIGENT SYSTEMS AND APPLICATIONS IN ENGINEERING
ISSN:2147-6799 www.ijisae.org Original Research Paper

Synthesis, Characterization, and Applications of Polyaniline-CdS Nanocomposites: A Comprehensive Review

Hodade Dipali Nagnath[1], Dr. Om Praksh Choudhary[2]

Submitted:01/05/2024 **Revised:**20/06/2024 **Accepted:**30/06/2024

Abstract: Polyaniline (PANI) is a widely studied conducting polymer due to its ease of synthesis, environmental stability, and unique doping mechanisms. This review explores recent advancements in the synthesis and characterization of PANI and its nanocomposites with cadmium sulfide (CdS). Various synthesis methods, including conventional, ultrasonic, and chemical polymerization, are discussed. Structural, optical, and electrical properties are examined using XRD, FTIR, SEM, and TEM analyses. The interaction between PANI and CdS significantly influences crystallinity, conductivity, and photocatalytic efficiency. These nanocomposites exhibit promising applications in sensors, supercapacitors, and photovoltaic devices. The review highlights future research directions to enhance the performance and stability of PANI-CdS-based materials for advanced technological applications.

Keywords: *Polyaniline, Conducting Polymers, Nanocomposites, Cadmium Sulfide, Polymerization, Photocatalysis, Electrical Conductivity, Sensors, X-ray Diffraction, FTIR Spectroscopy.*

1. Introduction

Polyaniline (PANI) is a conducting polymer with significant interest in electronics, energy storage, and sensing applications. Since its discovery, PANI has been extensively studied due to its simple synthesis, tunable electrical properties, and doping-dependent conductivity. The integration of cadmium sulfide (CdS) nanoparticles with PANI further enhances its electronic and optoelectronic capabilities. This review focuses on the synthesis techniques, structural characteristics, and functional applications of PANI-CdS nanocomposites. Special attention is given to their morphological modifications, crystallinity, and electrical performance. The goal is to provide a detailed understanding of these nanocomposites and their potential applications in modern technological advancements.

1Research Scholar, 2Associate Professor
1,2Department of Physics
1,2Dr. APJ Abdul Kalam University, Indore, MP, India
dipalihodade2@gmail.com
Corresponding author : Hodade Dipali Nagnath , dipalihodade2@gmail.com

The primary focus of this review study was on recent developments in the synthesis and characteristics of polyaniline conducting polymers. Research and development in the synthesis of polyaniline has been examined using a variety of processes, including the traditional technique, ultrasonic, the Fenton process, and substitution on the polyaniline backbone in the form of grafted polyaniline. A direct connection can be seen between the structure and the qualities when using this method of development, which achieves a high level of accuracy in its findings.

Polyaniline that has had its structure modified in a number of different ways might produce more interesting outcomes for use in the future. Polyaniline (PANI) is a semi-adaptable bar polymer conducting polymer (CP). Since the mid-1980s, mainstream scholars have scrutinized PANI. Polyaniline stands out among compound semiconductors (CPs) and natural semiconductors due to its easy combination, low environmental effect, and fundamental physics behind doping and de-doping. PANI production is straightforward, but its polymerization and oxidation mechanics are difficult. Polyaniline has been one of

the most studied conducting polymers for 50 years due to its broad scientific foundation.

Polyaniline is made by polymerizing aniline monomer and can have three romanticized oxidation states. Leuco-emeraldine is electron-free polyaniline. Imine rather than amine connections indicate fully oxidized pernigraniline. Polyaniline emeraldine base (EB) is neutral. It becomes emeraldine salt (ES) when doped, and an acid protonates the imine nitrogen's.

The most practical form of polyaniline is emeraldine base, which is stable at ambient temperature and electrically conductive after doping with acid.

Leuco-emeraldine and pernigraniline exhibit low electrical conductivity following acid doping.

Sensors and electro-chromic devices benefit from polyaniline's color shift in different oxidation states. Despite the importance of color, the best way to make a polyaniline sensor is to use the electrical conductivity changes between oxidation states or doping levels.

Polyaniline is usually formed through aniline oxidative polymerization. After dissolving aniline in HCl or another acid (the dopant), ammonium per-sulfate was added drop by drop as the oxidant; the reaction continued for two hours.

Special methods and dopants can recover polyaniline powder after polymerization. Dispersibility makes the powder beneficial for many applications. Three steps may arrange the emeraldine base. The reaction begins with pernigraniline salt (PS) oxidation. In the second stage, the pernigraniline molecule is oxidized to the radicalcation and reduced to the emeraldine salt. The final stage couples this radicalcation with ES salt.

Doped emeraldine salt polyaniline is electrically conductive and ideal for many applications. Electrically leading yarns, antistatic coatings, electromagnetic shielding, and changeable anodes are some examples. The electrochemical arrangement's position is also important. Polyaniline is used to make printed circuit boards (as a last completion) and erosion assurance. This makes polyaniline popular. Polyaniline is commonly created as long chain polymer totals, surfactant (or dopant) settled nanoparticle scatterings, or without stabilizer nano-fiber scatterings, depending on the planned course. Since the late 1990s, polyaniline scattering-cancelling surfactant or dopant has been sold.

PANI's unique features, which make it useful in many sectors, have driven interest in its study over the years. This high-performance polymer comes in mass powder, cast films, or filaments and is environmentally friendly and tunable. It's versatile since it's easy to make and mass-produced. Despite the fact that many papers have been published in the last five years, which would indicate that polyaniline is still the subject of much research, most of the fundamental portrayal of polyaniline has occurred in the last 20 years or so and is settled. Despite extensive research on polyaniline, this is true.

Polyaniline has an artificially modified -NH aggregate in a polymer chain bordered by phenylene rings. This phenylene-based polymer has an average molecular weight. Monomeric aniline particle 1, 4-coupling can also explain this behavior. NH-gathering proximity causes polyaniline protonation and de-protonation and other physico-concoction properties. Acidic aniline oxidative polymerization produces polyaniline. There are a few polyaniline findings in the literature on aniline polymerization structure and protection.

1.1 Synthesis of Polyaniline by Different Methods

1.1.1 Conventional method

The most frequent polyaniline combination is electrochemical or synthetic oxidative polymerization and doping. Electrochemical methods generate less.

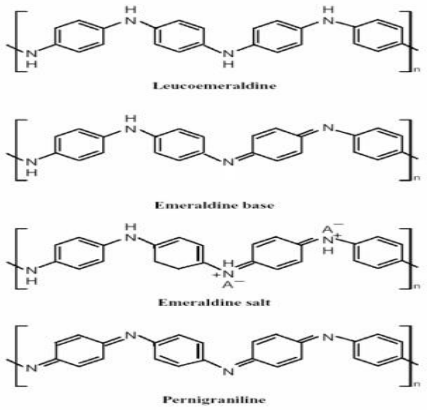

Figure1: Different oxidation states of polyaniline

Concoction oxidation with hydrochloric or sulfuric acid and ammonium per sulfate in water combines polyaniline. The oxidant removes a proton from an aniline atom without interacting with the substrate/intermediate or product. Letherby showed that redox interactions between the growing chain (oxidant) and aniline (reducer) with monomer expansion to the chain end increase the polymer chain. A solid oxidant, $(NH_4)2S_2O_8$, near the polymerization base enhances oligo and polyaniline oxidation.

Investigated aniline concoction oxidation with ferric chloride, $FeCl_3X6H_2O$, in HCl watery solutions for frame polyaniline powder found PANI/$Al2O_3$ using aniline, HCl, ammonium persulphate, and Al_2O_3; Cortes and Sierra developed the highest polyaniline by polymerizing aniline at appropriate temperatures, centralizing dode-cylbenzensulfonic acid (dopant), grouping ammonium persulphate (oxidant), and blending rate. 25°C, 27 mmol, 11.5 mmol, 500 rpm oxidative polymerized aniline with ammonium per-sulfate oxidant at 5°C to create camphor sulfonic acid (CSA)-doped polyaniline

Oxidative polymerization of aniline produces the most common polyaniline. Aniline was dissolved in HCl or other acids (dopant) and ammonium persulphate (oxidant) was added dropwise. Response was continued for two hours.

Polyaniline powder can be recovered after polymerization and made dispersible and used for many purposes using special polymerization processes and dopants. A three-phase emeraldine base show is suggested. The principal response forms the pernigraniline salt (PS) oxidation state. Pernigraniline is reduced to the emeraldine salt in the second stage as aniline monomer oxidizes to the radical cation. The third stage links this radical cation with ES salt.

Polyaniline is electrically conductive in the doped emeraldine salt form, making it suitable for electrically leading yarns, antistatic coatings, electromagnetic protection, and adjustable anodes. Its electrochemical configuration is also important. Polyaniline is used in printed circuit board manufacturing (as a last complete) and erosion assurance because it is more honorable than copper and less honorable than silver. Depending on the designed course, polyaniline is made as long chain polymer totals, surfactant (or dopant) settled nanoparticle scatterings, or stabilizer-free nano fiber scatterings. Since the late 1990s, surfactant or dopant-balanced polyaniline scatterings have been available for sale. The persistent interest in PANI research over the years is mostly due to its unique properties, which allow it to be used in various fields. It can be provided as mass powder, cast movies, or filaments. Its low-effort, large-scale creation makes it versatile. Despite the large number of papers published over the past five years, polyaniline's basic portrayal has been settled for at least 20 years.

Polyaniline is an average phenylene-based polymer with an artificially adapted – NH aggregate in a polymer chain flanked by phenylene rings. It is also monomeric aniline particle 1, 4-coupling. The proximity of the NH-gathering causes polyaniline's protonation and de-protonation and other physico-concoction features. Acidic aniline oxidizes to polyaniline. Polyaniline has been reported in writing about aniline polymerization structure and protection.

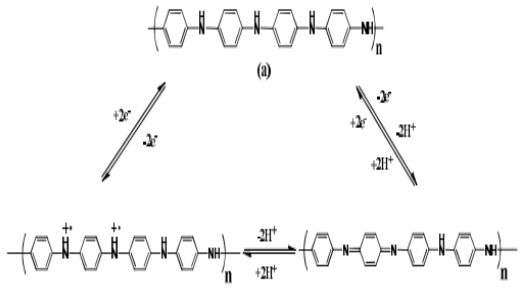

Figure 2: Different oxidation states of PANI and their conversion in each other (a) Leuco emeraldine Base (LEB) (b) Emeraldine salt (ES) (c) Emeraldine base (EB)

Table1 : XRD for PANI, CdS nanoparticles and PANI-CdS nanocomposites

Samples	2θ (deg.)	Plane (hkl)	FWHM (deg.)	Cryst. size (nm)	d (Aº)
PANI	25.75	110	1.05	7.95	3.45
CdS	26.69	002	0.925	12.09	3.33

PANI-CdS (10%)	25.72	100	1.25	6.64	3.46
PANI-CdS (20%)	25.54	100	1.158	7.01	3.48
PANI-CdS (30%)	25.45	100	1.176	6.84	3.49
PANI-CdS (40%)	25.75	100	1.885	4.42	3.45
PANI-CdS (50%)	25.05	110	0.50	15.90	3.55

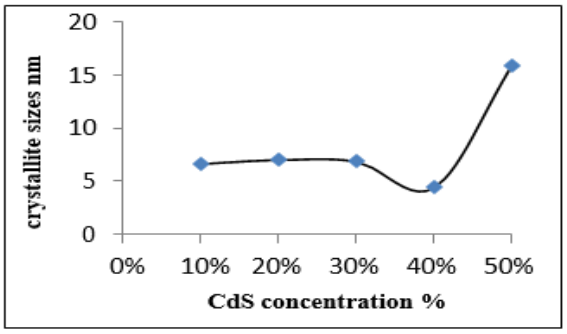

Figure 3: Shows the change of crystallite sizes with CdS concentration

PANI, CdS nanoparticles, and PANI-CdS nanocomposites were produced using straightforward techniques in order to examine their structural and morphological characteristics. The peaks of PANI and CdS appeared together in the PANI-CdS nanocomposites' X-ray diffraction pattern, indicating their interconnection, and the difference in their crystallite structures caused stress in the nanocomposites. The PANI matrix and CdS nanoparticles interact, according to FTIR. CdS nanoparticles are distributed uniformly throughout the PANI matrix, and AFM investigations have revealed that there is interconnectivity among them.

2. Literature Review

In this Paper Conductive polymer boost light absorption and photocatalytic electrons. CdS-ZnS and CdS-TiO2 precipitated PANI. Polyaniline improves photocatalysts (CdS, CdS-ZnS and CdS-TiO2). Measurements included charge transfer, molar ratio, surface form, particle size, diffraction pattern, and heat stability. Nano photo-catalyst PC, CZP, CTP is photo-catalysed. Nanotech enhances photocatalysis. Nanoparticle flaws capture weak CZP and CTP electron kinetics. Recombination reduces CdS-PANI photocatalysis. Photocatalytic water purification CZP, CTP, and CdS-Zn-TiO2 beat CdS-PANI [1].

PANI attaches photons. High-performance photocatalysts resulted. Nanotechnology degrades AB-29. Nanotechnology kills AB-29. Cadmium leaching prevents commercial CdS water cleansing. Sold cadmium polyaniline; Polyaniline photocatalysis, stability, reusability; Nano UV-to-IR (i.e., 340–850 nm) (i.e., 340–850 nm); Nanomaterials boost photocatalysis [2].

Cu-Al2O3-containing PANI-co-PPy was made in situ. Structure, temperature transition, and morphology were analyzed by FT-IR, XRD, DSC, and HR-TEM (HR-TEM). Novel electrical devices were created by testing AC conductivity and di-electricity at ambient temperature. FT-IR and XRD determined nanoparticle organization and synergy. HR-TEM shows nano-filled copolymer. GTT reduces polymer flexibility, according to DSC. Charge carrier hopping was observed in nanocomposites vs. virgin PANI-co-PPy. Dielectric 5wt% Cu-Al2O3 copolymer; nano-filler density improved nanocomposite dielectric characteristics. Al2O3 gas-sensing copolymer nanocomposites transmit electrons [3].

Unlike CdO NPs and Ag–CdO NCs, nanomaterials feature micron-scale grains. PANI-modified Ag–CdO NCs have FT-IR absorption peaks. CdO NPs and Ag–CdO NCs have sharp and strong XRD signals with reducing crystalline diameters. At pH 6, 10 ppm dye, 0.140 g catalyst load, and 210 min irradiation, Ag–CdO/PANI NCs degraded most efficiently [4].

In this research, we introduce a new hybrid design from POT-CSA and CdSe-TEA nanoparticles. Structure, morphology, and electricity are investigated. The hybrid material's XRD pattern is

cubic, like CdSe nanoparticles. The hybrid films are semiconducting, with a conductivity of 0.1 S.cm-2 [5].

In this Paper polymerizes in cadmium sulphide following ultrasonic irradiation (CdS). USI manufactures polymer/organic composites. PANI on CdS becomes PANI/CdS. USI nucleates particles. CdS concentration affects PANI/CdS particle size. PANI/CdS particles are created chemically, unlike USI. USI splits PANI/CdS. USI strengthens composite. PANI polymerization on CdS inhibits micro-fibre polymerization. XRD explains USI and validates PANI/CdS. After USI treatment, both materials kept their crystal structures but lost XRD crystallinity. TEM and SEM confirm XRD [6].

PANI study prompted merger. PANI is electrochemical and mechanical. It's vital to limit the reactions that generate PANI and its cheapest cost, then limit its use in nanocomposites with metals, their oxides, and/or carbon to determine what's lacking and broaden its chemistry. Advanced research focused PANI research. PANI's facile preparation and unique features attracted scientists. PANI comprises nanostructured metals, oxides, and carbon. 96Wh/kg power density, 8.88kW/kg energy density; Nano-PANI contributed. Nanostructure and conductivity make PANI a gas sensor. Nano-PANI improves gas sensor performance. This review covers polymer manufacturing, characteristics, nanocomposites, polymerization, and gas sensor applications [7].

PANI and CdS-QDs nanocomposites were morphologically, structurally, optically, and electrically characterized. CdS-PANI nanocomposites precipitated CdS QDs and polyaniline. UV eV is spectroscopy assessed PANI, CdS-PANI nanocomposites, and CdS quantum dots. Quantum dots change PANI's band gap. PANI and its nanocomposites showed 1-D charge transport in DC conductivity measurements. Temperature and CdS content improve CdS-PANI DC conductivity. CdS-PANI nanocomposites' AC conductivity depends on temperature, frequency, and CdS concentration [8].

COVID-19 required high-performance energy storage and anti-microbial technology due to energy crises, global warming, and pathogen contamination. Nanocomposites enhance renewable energy and environmental health.

In-situ oxidative polymerization generated nanotube-and-quantum-dot MCP nanocomposites. 1-MCP has higher super capacitance than f-MWCNT, 7-MCP, and 5-MCP. Carbon nanotubes and Polypyrrole have high conductivity, surface area, and stability, while cadmium sulphide quantum dots are electro-catalytic. A 24-hour ternary nanocomposite inhibited S. aureus and E. coli. MCP contains battery and antibacterial properties [9].

This page discusses water pollution adsorbents. Pollution and toxicity have been considered. We evaluate recovery and reuse, toxicity, research limitations, and SFNPs' prospects. SFNPs and derivative composites have unlimited Nano ferrites and their surface-modified composites are studied as waste water adsorbents. This review addresses SFNPs/SFNCs for organic and inorganic pollutant adsorption. Adsorption purifies wastewater simply, effectively, and cheaply. Adsorption isotherm, kinetic, thermodynamic, and mechanistic models are also studied. This report recommends waste water research [10].

Using APS as an oxidant, this study aims to create CdS-based PANI nanocomposites. We also analyze chemical structure, morphology, and electrical properties (FT-IR, XRD, DC conductivity). TEM determines nanoparticle shape and composition. Fore Probe measures CdS composite conductivity. Activation energy is calculated with different cds nanocomposite wt percentages and bulk Polyaniline [11].

Aniline oxidation yielded polyaniline powder. FT-IR spectroscopy revealed absorption peaks at 3498, 2858 cm^{-1}, corresponding to N-H vibrations and C-H expansion of the aromatic ring, as well as quinoid ring stretching vibrations. AFM and SEM measure surface topography and composition. Polyaniline powder pellets' structures were examined using analytical X-ray diffraction. Crystalline lines and three peaks were observed [12].

Polyaniline nanocomposite films were made utilizing aniline, ammonium per sulfate, and cdo. SEM techniques were used to study the development of Pani and Pani/cdo/ZnO composites. Pure Pani and its composites' DC conductivity was measured from 30 to 160°C. Emerging research links microbial extracellular electron transfer (EET) and photo

electrochemical processes to circumvent the disadvantages of solitary microbial or photocatalysis treatment; microorganisms use extracellular electron donors for respiration and acceptors to build a respiratory chain. EET-photo electrochemical technologies increase energy conversion efficiency, providing economic and environmental benefits. CdS NPs replace semiconductor photocatalysts. CdS NPs have the electrical conductivity, specific surface area, visible light-driven photocatalysis, and biocompatibility to promote hybrid microbial photo electrochemical processes [13].

This review examines photo electrochemical mechanisms. Future CdS NPs-based microbial-photo electrochemical applications are addressed. This research analyzes the usefulness of developed CdS NPs-bio-hybrids for environmental remediation and clean-energy production. Nano-size CuFe2O4 was generated by coprecipitation and 500°C calcination (CF). X-ray diffraction, FTIR, SEM, and photoluminescence spectroscopy on CF-Polyaniline nanocomposite; measuring CF-dielectric PANI's constant at different frequencies and temperatures. In water, CF-PANI eliminated Cr(VI). Contact duration, CF-PANI doses, Cr (VI) ion concentration, pH, and temperature affected Cr(VI) ion removal from aqueous solution. PH 2 absorbed most. Data fit Langmuir isotherm and pseudo-2nd order kinetic models [14].

3. Structural analysis of PANi, CdS and PANi–CdS nanocomposites

The XRD patterns of pure polyaniline in the emeraldine base form, cadmium sulphide (CdS) and PANi–CdS nanocomposites (10–50 wt%). The XRD pattern of PANi shows a broad peak at 2y¼25.301 which corresponds to (1 1 0) plane of PANi. This broad peak in the XRD pattern of PANi shows that it has some crystallinity. The crystallinity of PANi can be ascribed to the repetition of benzenoid and quinoid rings in PANi chains.

The XRD patterns of nano CdS, PANi–CdS (10–50 wt%) nanocomposites exhibit the characteristic peaks for crystalline CdS of hexagonal wurtzite structure. This indicates the crystal structure of CdS is not modified due to the presence of PANi. The diffraction peaks in XRD patterns of nano CdS powder and PANi–CdS (10–50 wt%) nanocomposites have been indexed to the hexagonally wurtzite structured CdS which are consistent with the standard values for CdS given in JCPDS file (80–006).

The increase in lattice parameters indicate a slight stretching of unit cell of CdS due to the adsorption of PANi molecular chains on the surface of the CdS. The presence of such interaction can also be studied by the crystal aspect ratio which is defined as the ratio of crystallite size in the (1 0 1) and (0 0 2) planes of X-ray diffraction pattern. The crystallite sizes of CdS, PANi–CdS (10–50 wt%) nanocomposites for three prominent peaks (1 0 0), (0 0 2) and (1 0 1) are calculated by Scherrer formula.

The crystallite sizes of CdS in (1 0 0), (0 0 2) and (1 0 1) planes decrease by 21.24, 29.46 and 13.86% in PANi– CdS (10–50 wt%) nanocomposites. This decrease in crystallite sizes of CdS in PANi–CdS (10–50 wt%) nanocomposites shows that the crystallinity of CdS is disturbed by the adsorption of PANi molecular chains on the surface of CdS. For PANi–CdS (10–50 wt%) nanocomposites, the crystal aspect ratio increases by 15.16 and 41.64% in comparison of the pure CdS. These results indicate the interaction between the CdS nano particles and PANi molecular chains due to the adsorption of PANi molecular chains on the surface of the CdS

3.1 Instrumentation

Powder X-ray diffraction pattern of the nanoparticles was obtained using a powder X-ray diffractometer (PANalytical Model, Nickel filtered Cu K α radiations with λ= 1.54056 Å at 35 kV, 10 mA). The sample was scanned over the required range for 2Ɵ values (10-70^{o}). The FTIR spectrum of the sample was recorded using a Shimadzu 8400S spectrometer by the KBr pellet technique in the range 400- 4500 cm^{-1}. The SEM images of the synthesized samples were recorded using a Hitachi Scanning Electron Microscope.

The size and shape of nanoparticles was obtained by high resolution transmission electron microscopy (HRTEM) and HRTEM measurements were carried out on a JOEL JEM 2000.

Table 2 : DC conductivity and activation energy for pure PANI and PANI/CdS.

Sr. No.	Material	Conductivity'σ (S/cm)	Activation energy, Ea(eV)
1.	Pure PANI	$2.705X10^{-2}$	$3.97X10^{-4}$
2.	5% PANI/CdS	$8.22\ X10^{-2}$	$2.13X10^{-4}$
3.	10% PANI/CdS	$7.974\ X10^{-2}$	$1.2065X10^{-4}$
4.	15% PANI/CdS	$2.835\ X10^{-1}$	$1.226X10^{-4}$
5.	20% PANI/CdS	1.40224	$0.9191X10^{-4}$
6.	25% PANI/CdS	1.96766	$0.6786X10^{-4}$

3.2 Conductivity

Directing polymers will be polymers containing a broadened pi conjugated framework, made up of cover of independently possessed p - orbitals in the foundation of the polymer chain. In spite of the fact that directing polymers have a generally extensive number of delocalized pi electrons, a genuinely expansive vitality hole exists between the valence band and the conduction band (more noteworthy than 1 eV), in this manner these polymers are viewed as semi-leading. These polymers must be doped (generally significance modifying the quantity of pi electrons) with the end goal to render the polymers genuinely directing.

Doping the polymers makes new states (contributor or acceptor states), which exist inside the band hole and are vigorously available to the pi electrons, bringing about huge increment in conductivity.

Truth be told, the conductivity of doped polymers might be up to ten requests of greatness more prominent than that of the unbiased (undoped) polymers. The idea of conductivity of conjugated polymers was immediately widened from polyacetylene to incorporate a conjugated hydrocarbon and fragrant heterocyclic polymers, for example, poly (p-phenylene) and polythiophene. The conductivity of different doped and undoped polymers, some regular semiconductors and metals are introduced in Table 3.2

Table 3: Conductivity of various doped and undoped polymers, some common semiconductors and metals

Material	Conductivity (S/Cm)
Gold, Silver, Copper	$\sim10^{6}$
Doped trans- polyacetylene	$\sim10^{5}$
Doped polyaniline	$\sim10^{1}$
Germanium	$\sim10^{-2}$
Silicon	$\sim10^{-6}$
Undoped trans-polyacetylene	$\sim10^{-6}$
Undoped polyaniline	$\sim10^{-10}$
Glass	$\sim10^{-10}$
Quartz	$\sim10^{-12}$
H_2SO_4 doped polyaniline	$\sim10^{-8}$
Dodecylbenzene sulfonic acid-doped Polyaniline	$\sim10^{-8}$

As the directing polymers might be doped to different degrees, there is a component of control in doping level, consequently the conductivity. This capacity to tailor the polymer's electrical properties embodies the flexibility of directing polymers.

3.3 Optic features

The optical properties of polymers include refractive record, reflection, scrambling, ingestion, clarity, shine, murkiness, birefringence, push optic coefficient, photochemical When contemplating the versatility of a polymer for usage in a variety of contexts, it is

essential to take into account the optical properties of the material in question. This is due to the fact that one must take into consideration the optical qualities of the material. One example of this kind of use is seen in the focal points of spectacles; other examples include smaller circular coatings and the packaging of food and beverages. When deciding the value of a polymer to be used as a plate covering, one of the most significant factors to take into account is the pressure optic coefficient. This is because the pressure optic coefficient serves to decide how successfully the polymer will attach to the plate. Because of the pressure optic coefficient, this is the case.

Table 4: Absorption bands of synthesized PANIs samples

Absorption bands (cm^{-1}) Synthesized PANIs samples				
	PANI -NP	**PANI -NFR**	**PANI -NFS**	**PANI -NR**
Quinoid ring stretching vibrations	1587.3	1589.2	1571	1576.6
Benzenoid ring stretching vibrations	1502.5	1508.2	1475.5	1479.3
C–N stretching vibrations	1303.8	1307.6	1299.8	1305.7
C–H in-plane bending vibrations	1143.7	1151.4	1134.1	1136.4
N–H stretching vibrations	3456.2	3460.1	3460	3462.1
C–H out of plane bending vibration	831	836.1	806.6	808.3

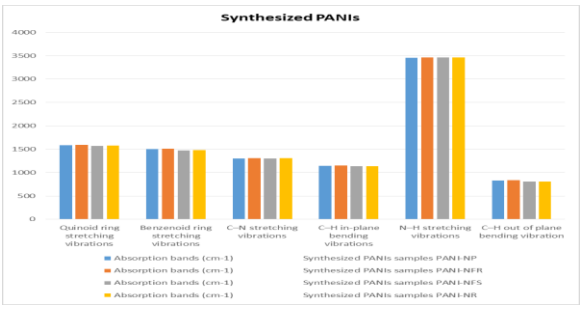

Figure 4: Absorption bands of synthesized PANIs samples

The synthesized PANIs four samples' absorption characteristic bands are shown in Table 5 The sol gel-prepared PANI-NP characteristic peaks matched those of I-prepared PANI granules.

Table 5: Surface area, total pore volume and average pore diameter of PANIs samples

Synthesis method	**Surface area (m^2/g)**	**Total pore volume (cm^3/g)**	**Average pore size (nm)**
PANI-NP	20.782	0.0294	14.566
PANI-	33.37	0.084	10.107
NFR	34.59	0.985	12.63
PANI-NFS	35.085	0.099	11.292
PANI-NR	24.61	0.0336	5.466

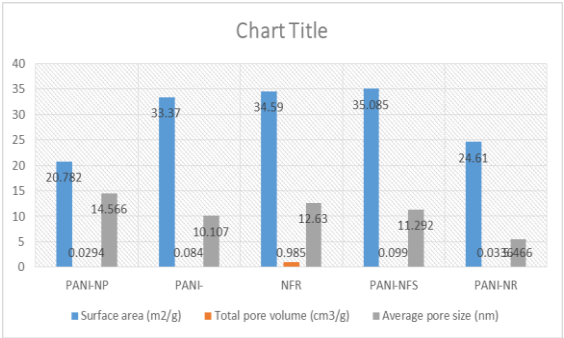

Figure 5: Surface area, total pore volume and average pore diameter of PANIs samples

Table 5 shows the BET surface area, total pore volume, and average pore size of prepared PAN-NP, NFR, NFS, and NR. PANI-NF (made by fast mixing or sonochemical polymerization) has a greater surface area and total pore volume than PANI-NP and PANI-NR. The sono-assisted synthesis polyaniline had a lower BET surface area value (22.38 m2/g) than PANI-NFR (33.37 m2/g), PANI-NFS (35.085 m2/g), and PANI-NR (24.61 m2/g).

FTIR results of synthesized nanofibers by rapid mixing and ultra-sonic polymerization show a shift from 1589.2 cm^{-1} to 1571 cm^{-1} assigned to high doping level and conductivity, which matches SEM images of thinner and uniform nanofibers prepared by ultra-sonication, research found similar values of characteristic peaks of nanofibers, although the tiny differences between these values and PANI-NFR and PANI-NFS may be attributed to synthesis method changes.

For PANI-NR, the distinctive peaks in the table were similar to nanorods prepared by Haibing Xia et al. due to the change in production technique and the presence of hydrophilic Allura Red as a structure-directing agent.

3.4 Tensile strength to its absolute limit

The variation in ultimate tensile strength is depicted in Figure 8 as a function of the amount of CdS filler. The final tensile strength found at break varied with increasing filler quantities, and a tendency comparable to this was reported in other places. When compared to clean PVA, the observed values indicate that the tensile strength of polymer nanocomposites is significantly improved across the board for all concentrations of filler. Therefore, it is possible to say that the mechanical properties of composites gain higher reinforcement as a result of the dispersion of nano CdS particles in the matrix. This can be attributed to greater surface area as well as multiple interactions involving various functional groups of the matrix and the filler in the composites. When the amount of CdS in the polymer composite was raised, the tensile strength first improved dramatically and then continued to grow at higher CdS loadings.

Table 6: Range of values for measured thermal properties of PVA/CdS nanocomposites

Temperature,	Units		CdS Content (wt.%)				
CDS Content in PVA (WT.%)	-	-	0	0.5	1.0	1.5	2.0
Heat of Fusion,	ΔH	J/g	40.54	40.89	41.49	37.29	35.72
Percentage	%xc	%	4.39	5.768	4.572	4.408	4.171
Glass Transition	Tg	0C	81.6	71.3	68.4	71.2	69.2
Melting Temperature	Tm	0C	226.8	179.3	189.2	195.6	199.5

The terms "true stress" and "true strain" are utilized in the computation of toughness. The embedding of nanoparticles is thought to be responsible for the morphological and structural changes that lead to an increase in toughness. According to the findings of this study, the composite film with 2% nano CdS had the highest level of toughness.

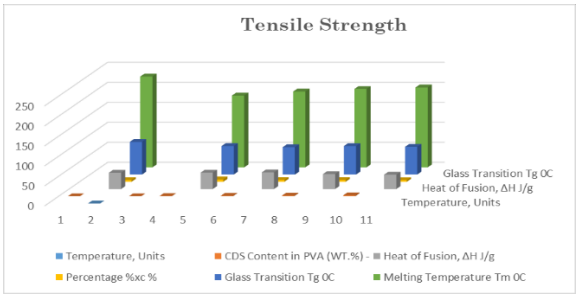

Figure 6: Range of values for measured thermal properties of PVA/CdS nanocomposites

The significant increase in toughness that was observed in nano-composite films of PVA/CdS in this work is calculated in Table 6 and depicted. When compared to that of pure PVA film, the nano CdS/PVA film with 2% filler demonstrated the greatest gain in toughness (710 percent more than the pure PVA film). Tensile testing was performed on the samples of PVA

and PVA/CdS nano composites in an effort to break them apart. Figure 6 depicts the stress and strain curves of both pure PVA and a nanocomposite film that was created using the nanocomposite. There was a unique pattern that appeared across all of the films, and it was this: the stress level increased with the addition of CdS nanoparticles, which is indicative of the function of these nanoparticles as a reinforcement.

The composites exhibit a linear stress–strain character up to the point of failure and plastic deformation. Additionally, the composites confirm a comparable curve shape for both plain and nano filler composites. After being subjected to the treatment, each of the samples exhibited an increase in both their tensile strength and their modulus values.

4 XRD validates PANI/CdS' crystal structure

XRD validates PANI/CdS' crystal structure. SEM and XRD demonstrate composites' changed crystallinity. CdS crystallites develop and impregnate PANI's granular pillar-like structure. The composite absorbs bluer than CdS. PANI's C=C bond alters infrared wave numbers. PANI switches between base and salt states quickly. PANI has good reduction and oxidation properties, electrical conductivity, a simple manufacturing method, and environmental stability. PANI was oxidatively polymerized from aniline monomers. Different approaches were utilized as PANI research progressed.

- Polymerization using electrochemistry.
- Polymerization by chemicals.
- Polymerization in the vapor phase (VPP).
- Polymerization that was started by photochemistry.
- Polymerization facilitated by enzymes.
- Electron acceptor-based polymerization

4.1 Material & Techniques

4.1.1 Polyaniline synthesis

Polyaniline was made through oxidative polymerization. In a beaker, 0.2M (0.8 g) aniline, 2 M HCl, and distilled water were mixed. Beaker in (0-8) oC ice bath. The glass substrate was dipped. Ammonium peroxydisulfate was dissolved in 2 M HCl and purified water. Drop by drop, ammonium peroxydisulfate was added to aniline while stirring. The mixture turns from light blue to blue green to greenish black during polymerization. Color denotes emeraldine salt polyaniline. We kept this overnight. Filtered and rinsed with HCl and distilled water to eliminate contaminants. The residue and substrate were dried at 80°C for 4 hours. Polyaniline, a conducting polymer, has several uses. This conducting polymer is likely produced in rings and nitrogen-substituted derivatives. The technological potential of these materials depends on their cost-effectiveness, stability, and ease of synthesis and processing.

4.1.2 Cadmium-sulfide synthesis

80 ml distilled water dissolved 6.396 mg cadmium acetate and 3.648 g thiourea. Drop by drop, thiourea solution was added to the cadmium acetate solution while stirring. After 3.5 h, nanoparticles precipitate and the solution turn yellow. The solution sat overnight without stirring.

4.2.3 Nanocomposite PANI–CdS

This study analyses iodine's effect on polymer/inorganic nanocomposites. I2@PANI is redox-coated iodine nanoparticles on PANI nano-fibers. CdS nanoparticles increase I2@PANI–CdS photocurrent (as electron acceptors). I2's penetration into porous semiconductor sheets, quick charge transfer, and slow photoelectron recombination all help. Nano-CdS may have more charge carriers. I2@PANI–CdS nanocomposites boost photocurrent. XRD confirms a PANI/CdS composite's crystalline structure. SEM and XRD show the composites' altered form and crystallinity. Transmission electron microscopy shows CdS crystallites growing and impregnating PANI's granular pillar-like structure. The composite's absorption edge is blue-shifted compared to CdS. PANI's C14C bond strengthens, causing a shift in infrared wave numbers.

The first in-situ oxidative polymerization of polyaniline-CdS nanocomposite was performed.

This study used hybrid POT-CSA-CdSe-TEA nanoparticles. Studying electricity, structure, and morphology. XRD hybrids are cubic like CdSe nanoparticles. Semiconducting hybrids conduct 0.1 S.cm-2. This paper polymerizes ultrasonic-irradiated cadmium sulphide. USI makes organic-polymer composites. PANI/CdS. This USI creates particles.

Concentration controls PANI/CdS particle size. USI is not chemically made like PANI/CdS. USI splits PANI/CdS. USI strengthens composite. CdS PANI blocks micro-fibre polymerization. Discover USI and XRD-verified PANI/CdS. Both materials retained crystal structures but lost XRD crystallinity after USI. TEM and SEM confirm XRD.

PANI and CdS-QDs nanocomposites were examined for optics, electronics, morphology, and structure. CdS-PANI nanocomposites precipitate QDs and polyaniline. The UV eV spectroscopy examined PANI, CdS-PANI nanocomposites, and CdS quantum dots. Quantum dots modify PANI's band gap. PANI and nanocomposites showed 1-D charge transport in DC conductivity measurements. CdS-PANI DC conductivity rises with CdS and temperature. AC conductivity of CdS-PANI nanocomposites depends on temperature, frequency, and CdS content. This study creates CdS-based PANI nanocomposites with APS as an oxidant. Chemical structure, morphology, and electrical properties are studied. Nanoparticle form and content are determined by TEM. Fore Probe measures CdS composite conductivity. Calculating activation energy with polyaniline and various CdS nanocomposite weights. Others require superfluous steps, whereas enzyme-catalysed polymers are well-structured. Process and dissolve with templates. Polyelectrolyte templates foster para coupling and counterion doping. This study analyses new polyaniline conducting polymer synthesis and properties. Traditional, ultrasonic, Fenton, and grafting polyaniline synthesis methods are addressed. Highly accurate evolution links structure and characteristics.

4.2.4 Potential of structure-modified polyaniline.

Optoelectronics, morphology, and PIn/CdS nanocomposite structure are reported. FT-IR and XRD found CdS in PIn. TEM and FESEM examined synthesized samples. Nanocomposite PIn/CdS 2.15 eV optical band gap; PL spectra electron-hole mobility. The J-V characteristics of PIn/CdS nanocomposite Ohmic conductance were examined. Each statistic shows optoelectronic PIn/applicability CdSs. PVA had CdS nanoparticles. PVA/CdS nanocomposite films examined CdS nanoparticles' effects on PVA. We examine mechanical and structural properties. FTIR peaks show C-H, CO, COC, and COS stretching; XRD shows 100% nano-CdS. SEM pictures of PVA/CdS nanocomposite showed nanoparticle agglomeration. We measure thermal characteristics with DSC. Many electroactive polymers use. Conductive polymer PANI is easy to make. PANI LEDs light. Low-cost PANI solar cells. PANI solar cells are affordable and efficient. PANI gas and glucose sensors are popular. Increase energy efficiency with supercapacitors. Super capacitors use PANI's cost, conductivity, and redox. Medicine needs new tech. Neuroprotective brain probes improve neurology.

Table 7: Weight loss (%) at various temperatures for the as-prepared materials

Specimen	Weight loss (%) 30- 300 ^{0}C	Weight loss (%) 350- 650 ^{0}C	Weight loss (%) 650- 950 ^{0}C	Net Weight loss (%)
PANI	21.41	25.56	14.09	58.96
PANI/CdS	19.71	18.05	20.68	55.62
PANI/CdS	18.95	16.61	22.31	52.98

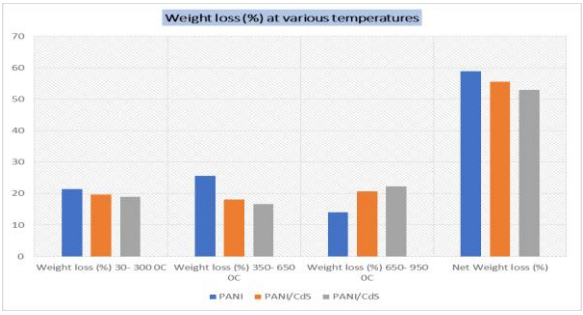

Figure 7: Weight loss (%) at various temperatures for the as-prepared materials

Video and probable PANI/CdS analysis in situ. XRD, FTIR, and SEM evaluated structure, shape, crystallinity, composition, and molecular interaction. Based on AC frequency, nanocomposite CdS enhances conductivity, dielectric, and impedance. Percolation changes PANI/CdS. P3 composite dielectric is low. CdS nanoparticles impact electric composites. Conductive hybrid polymers store energy.

Table 8: Ohmic conductance and resistance of the as-prepared samples

Sample	Ohmic Conductance (S)	Ohmic Resistance (Ω)
CdS	0.078	19.85
Neat PANI	0.089	14.59
PANI/CdS	0.101	11.37
PANI/Gradient/Cds	0.392	04.82

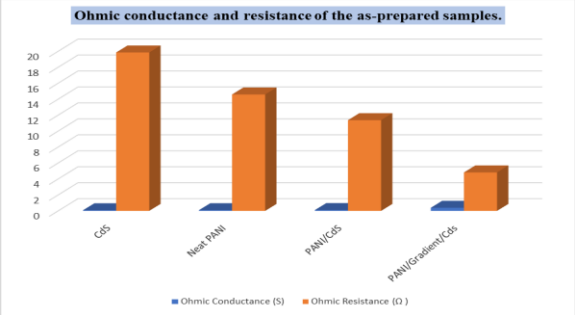

Figure 8: Ohmic conductance and resistance of the as-prepared samples

Biosensor matrix clad. Cross-linked glucose oxidase. Certified nanocomposite by XRD/FE-SEM. Sensor nanocomposite matrix was optically imaged. A glucose sensor. Biomolecules stick to fibre optic sensors with PANI-CdS.

4.3 Summary of the parameters extracted from the devices with different cadmium concentrations.

Table 9: Parameters extracted from the devices with different cadmium concentrations

$CdCL_2$ Concentration	Resistance (KΩ	Isc (μA)	Voc (mV)	FF (%)	Efficiency
3.8	4.1	8.9	91	35	0.0389
7	7.9	11	278	32	0.01156
8.9	11.5	38	478	39	0.1098
12	4.6	38	395	49	0.425
14.9	5.8	43	294	37	0.783

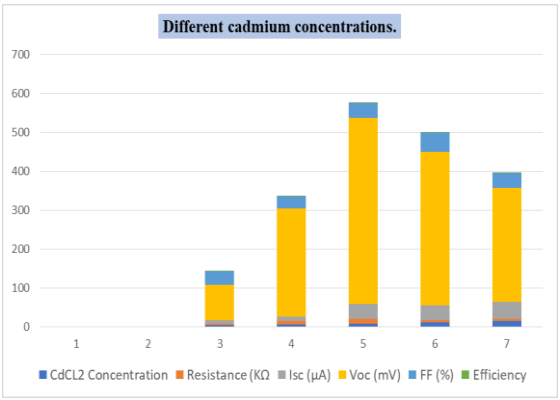

Figure 9: Parameters extracted from the devices with different cadmium concentrations.

The photovoltaic characteristics that were acquired by adjusting the polymerization time, the concentration of cadmium, and the concentration of dopant. The parameters that were acquired from the devices that contained varied amounts of cadmium are summarized below for your convenience.

4.4 Summary of the parameters extracted from the devices with different polymerization times.

For your convenience, the parameters that were obtained from the devices that contained varying quantities of cadmium are summarized here. These variables were obtained from the devices. The parameters that were acquired from the devices that exhibited different polymerization periods are summarized in the next paragraphs.

Table 10: Parameters extracted from the devices with different polymerization times.

Time	Resistance (KΩ	Isc (μA)	Voc (mV)	FF (%)	Efficiency
100	7.8	40	180	16	0.0986
200	11	45	440	40	0.086
300	39	365	520	29	0.78
400	41	105	899	30	0.64
500	52	98	564	35	0.15

The output current (Isc) also increased as the concentration of CdS increased, which may be owing

to an increase in defects and, as a result, an increase in light absorption and photon conversion.

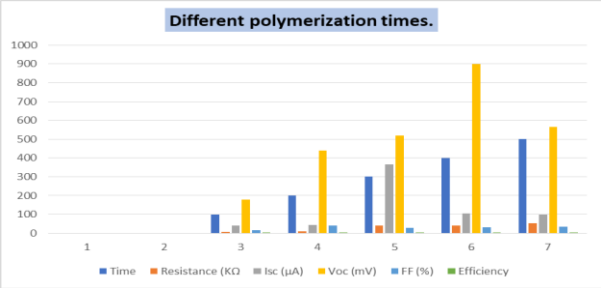

Figure 10: Parameters extracted from the devices with different polymerization times.

Nanoparticles provide a high interfacial surface for charge separation and reduced recombination, whilst polyaniline can be modified to have certain electrical characteristics and a band gap that can be tailored to the specifications of the device. Through the use of photo-electrochemical research, this composite has demonstrated the potential to be utilised in photovoltaic applications. An IPCE value of 11.2% was obtained by photocurrent studies, which revealed a high photon conversion efficiency when exposed to light environments. There will be an improvement in device response if effective solutions for matrix alignment are developed.

5. Conclusion

Polyaniline-CdS nanocomposites exhibit remarkable potential in optoelectronic and energy storage applications. Their unique structural, electrical, and optical properties make them suitable for use in sensors, supercapacitors, and photovoltaics. The synthesis methods significantly influence crystallinity, conductivity, and material stability. Characterization techniques such as XRD, FTIR, SEM, and TEM confirm strong interactions between PANI and CdS, leading to enhanced charge transport and reduced recombination rates. Despite extensive research, challenges remain in optimizing stability and improving large-scale synthesis. Future work should focus on developing environmentally friendly processing methods and enhancing material properties for commercial applications. This study underscores the versatility of PANI-CdS nanocomposites in advancing modern materials science.

References

[1] Qutub, N., Singh, P., Sabir, S., Umar, K., Sagadevan, S. and Oh, W.C., 2022. Synthesis of polyaniline supported CdS/CdS-ZnS/CdS-TiO2 nanocomposite for efficient photocatalytic applications. *Nanomaterials*, *12*(8), p.1355.

[2] Sankar, S. and Ramesan, M.T., 2022. Synthesis, characterization, conductivity, and gas-sensing performance of copolymer nanocomposites based on copper alumina and poly (aniline-co-pyrrole). *Polymer Engineering & Science*, *62*(8), pp.2402-2410.

[3] Alemu, T., Taye, G., Asefa, G. and Merga, L.B., 2022. Surface modification of Ag–CdO with polyaniline for the treatment of 3′, 3 ″, 5′, 5 ″-tetrabromophenolsulfonphthalein (BPB) under UV-visible light irradiation. *Heliyon*, *8*(11).

[4] Mohammeda, K.A., Ziadanb, K.M., AL-Kabbib, A.S. and Zabibahc, R.S., 2022. Novel POT/CdSe blend for optoelectronic applications. *Chalcogenide Letters*, *19*(9), pp.621-626.

[5] Ingle, R.V., Kaur, J., Lokh, P.E., Tabhane, V.A. and Pathan, H.M., 2022. Effect of ultrasonic irradiation treatment on the composites of polyaniline/cadmium sulfide. *ES Materials & Manufacturing*, *18*(3), pp.18-24.

[6] Majeed, A.H., Mohammed, L.A., Hammoodi, O.G., Sehgal, S., Alheety, M.A., Saxena, K.K., Dadoosh, S.A., Mohammed, I.K., Jasim, M.M. and Salmaan, N.U., 2022. A review on polyaniline: synthesis, properties, nanocomposites, and electrochemical applications. *International Journal of Polymer Science*, *2022*(1), p.9047554.

[7] Rasool, A., Rizvi, T.Z., Nayab, S. and Iqbal, Z., 2021. Electrical properties of Cadmium Sulfide quantum dots and polyaniline based nanocomposites. *Journal of Alloys and Compounds*, *854*, p.156661.

[8] Al Dalaeen, J.H., Khan, Y. and Ahmad, A., 2021. Synthesis and application of nanocomposite reinforced with decorated multi walled carbon nanotube with luminescence quantum dots. *Advances in Nanoparticles*, *10*(2), pp.75-93.

[9] Dhiman, M., Kaur, B. and Kaur, B., 2021. Application of magnetic nano particles and their composites as adsorbents for waste water

treatment: a brief review. *Ferrite: Nanostruct. Tunable Prop. Diverse Appl*, *112*, pp.246-278.

[10] Bhaiswar, J.B., Meghe, D.P., Salunkhe, M.Y. and Dongre, S.P., Synthesis, DC Electrical Conductivity and Activation Energy of Metal Sulphides Doped Polyaniline-Nanocomposite.

[11] Hasoon, S.A. and Abdul-Hadi, S.A., 2020. Chemical Synthesis and Characterization of Conducting Polyaniline. *Baghdad Science Journal*, *17*(1), pp.106-111.

[12] Husain, J., Anjum, R., Mathad, G., Pathar, D., Sagar, J. and Anjum, B., 2020. Electrical properties of polyaniline/Cadmium Oxide/ZnO Nanocomposites Thin Films. *International Research Journal on Advanced Science Hub*, *2*(08), pp.31-33.

[13] Dong, G., Wang, H., Yan, Z., Zhang, J., Ji, X., Lin, M., Dahlgren, R.A., Shang, X., Zhang, M. and Chen, Z., 2020. Cadmium sulfide nanoparticles-assisted intimate coupling of microbial and photoelectrochemical processes: Mechanisms and environmental applications. *Science of the Total Environment*, *740*, p.140080.

[14] Taddesse, A.M., Bekele, T., Diaz, I. and Adgo, A., 2021. Polyaniline supported CdS/CeO2/Ag3PO4 nanocomposite: An “AB” type tandem nn heterojunctions with enhanced photocatalytic activity. *Journal of Photochemistry and Photobiology A: Chemistry*, *406*, p.113005.